13th World Conference on Earthquake Engineering
Vancouver, B.C., Canada
August 1-6, 2004
Paper No. 538

# DEEP $V_S$ PROFILING ALONG THE TOP OF YUCCA MOUNTAIN USING A VIBROSEIS SOURCE AND SURFACE WAVES

**Kenneth H. STOKOE, II[1], Brent L. ROSENBLAD[2], Ivan G. WONG[3], James A. BAY[4]**
**Patricia A. THOMAS[5], and Walter J. SILVA[6]**

## SUMMARY

Yucca Mountain, Nevada, was approved as the site for development of the geologic repository for high-level radioactive waste and spent nuclear fuel in the United States. The U.S. Department of Energy has been conducting studies to characterize the site and assess its future performance as a geologic repository. As part of these studies, a program of deep seismic profiling, to depths of 200 m, was conducted along the top of Yucca Mountain to evaluate the shear-wave velocity ($V_S$) structure of the repository block. The resulting $V_S$ data were used as input into the development of ground motions for the preclosure seismic design of the repository and for postclosure performance assessment. The noninvasive spectral-analysis-of-surface-waves (SASW) method was employed in the deep profiling. Field measurements involved the use of a modified Vibroseis as the seismic source. The modifications allowed the Vibroseis to be controlled by a signal analyzer so that slow frequency sweeps could be performed while simultaneous narrow-band filtering was performed on the receiver outputs. This process optimized input energy from the source and signal analysis of the receiver outputs. Six deep $V_S$ profiles and five intermediate-depth (about 100 m) profiles were performed along the top of Yucca Mountain over a distance of about 5 km. In addition, eleven shallower profiles (averaging about 45-m deep) were measured using a bulldozer source. The shallower profiles were used to augment the deeper profiles and to evaluate further the near-surface velocity structure. The $V_S$ profiles exhibit a strong velocity gradient within 5 m of the surface, with the mean $V_S$ value more than doubling. Below this depth, $V_S$ gradually increases from a mean value of about 900 to 1000 m/s at a depth of 150 m. Between the depths of 150 and 210 m, $V_S$ increases more rapidly to about 1350 m/s, but this trend is based on limited data. At depths less than 50 m, anisotropy in $V_S$ was measured for surveys conducted parallel and perpendicular to the mountain crest, with the velocity parallel to the crest about 200 m/s higher. In the 5- to 50-m depth range, the average coefficient of variation (COV) of all data is about 0.25. Below 75 m, where the data set is smaller and includes measurements only parallel to the crest, the average COV decreases to a value of about 0.11.

## INTRODUCTION

[1] University of Texas at Austin, TX 78712, USA, Email: k.stokoe@mail.utexas.edu
[2] University of Missouri-Columbia, MO 65211, USA, Email: rosenbladb@missouri.edu
[3] URS Corporation, Oakland, CA 94607, USA, Email: Ivan_Wong@urscorp.com
[4] Utah State University, Logan, UT 84322, USA, Email: jim.bay@usu.edu
[5] URS Corporation, Oakland, CA 94607, USA Patricia_Thomas@urscorp.com
[6] Pacific Engineering Analysis, El Cerrito, CA 94530, USA, Email: pacificengineering@juno.com

Yucca Mountain, Nevada, was approved as the site for development of the geologic repository for the disposal of high-level radioactive waste and spent nuclear fuel in the United States. For more than 20 years, the U.S. Department of Energy has studied Yucca Mountain to characterize the site and assess its future performance as a geologic repository. As part of these studies, a comprehensive program of geotechnical, geological, and seismic investigations has been performed to characterize the repository block. The repository block is the portion of Yucca Mountain that contains the emplacement area and includes the subsurface geology from the mountain crest to depths below the proposed waste emplacement area which will be located at a depth of about 300 m. The purpose of the investigations has been to characterize the geologic and velocity structures of the repository block and the nonlinear dynamic material properties of the various geologic units. The results of the seismic investigations discussed in this paper were used to develop a basecase shear-wave velocity ($V_S$) profile for the mountain, including uncertainty. The profile was then used as input into the site response analysis to compute the ground motions for the preclosure seismic design and postclosure assessment.

In situ seismic velocity measurements were performed at 22 locations on top of Yucca Mountain using the spectral-analysis-of-surface-waves (SASW) method. The SASW surveys were aimed at evaluating: (1) the top 150 to 200 m of the mountain above the emplacement area, (2) an apparent $V_S$ gradient in the near surface (within about 5 to 15 m), and (3) any lateral variability over the footprint of the emplacement area. The SASW surveys provided spatial coverage on top of the mountain in a cost effective and environmentally friendly manner since no boreholes had to be drilled and no new roadways or work areas had to be constructed.

In this paper, the site geology at Yucca Mountain is briefly described. The methodology and approach used to collect $V_S$ data based on the SASW method are then described. Finally, the $V_S$ profiles, consisting of eleven deep profiles (up to 210 m in depth) and eleven shallower profiles (averaging about 45-m deep), are then presented and discussed.

## SITE GEOLOGY

Yucca Mountain is located in southern Nevada, within the Great Basin which is part of the Basin and Range structural/physiographic province. Pre-Tertiary rocks, consisting of a thick sequence of Proterozoic and Paleozoic sedimentary rocks, underlie approximately 1,000 to 3,000 m of Miocene volcanic rock in the Yucca Mountain area [1]. The mountain is an irregularly shaped upland, 6 to 10 km wide and about 35 km long. The crest of Yucca Mountain is at an average elevation of about 1,500 m (Figure 1). Elevation of the ground surface in the region ranges from about 900 m southeast of the site, in the lower reaches of Forty Mile Wash, to over 1,830 m about 6 km to the north, in the area of the Timber Mountain caldera.

Yucca Mountain consists of stacked layers of tuffs (Figure 1). The tuffs are approximately 7.5 to 15 million years old, and were formed by eruptions of volcanic ash from the north. Individual layers of volcanic tuff, therefore, get progressively thinner from north to south. Most of the rocks are welded and nonwelded ash flow tuffs [1]. As the ash settled, it was subjected to various degrees of compaction and fusion, depending on the temperature and pressure. When the temperature was high enough, ash was compressed and fused to produce a welded tuff, a hard, dense, brick-like rock with very little open pore space in the rock matrix. Nonwelded tuffs occur between the layers of welded tuff. These tuffs are

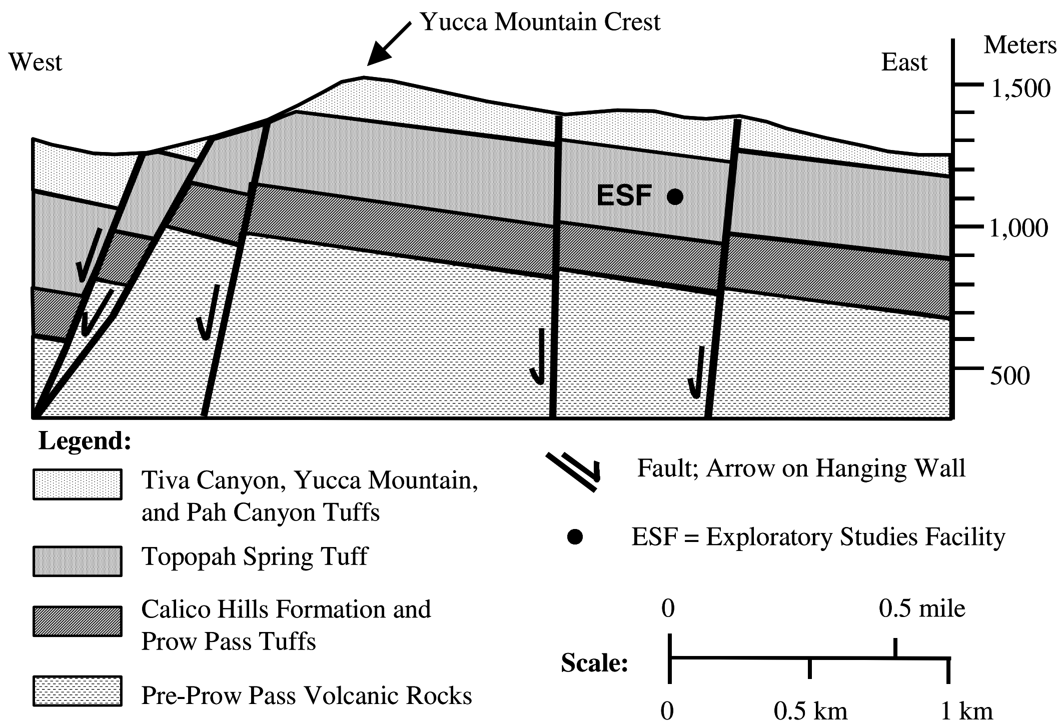


**Figure 1 Simplified geologic cross-section of Yucca Mountain**

compacted and consolidated at lower temperatures, are less dense and brittle, and have a higher porosity. The composition of the rocks at Yucca Mountain ranges from rhyolite to dacite or latite.

## OVERVIEW OF THE SASW METHOD

The SASW method is a stress-wave based method to nondestructively and nonintrusively determine the $V_S$ profile of a material [2]. The method utilizes the dispersive nature of Rayleigh-type surface waves propagating through a layered material. In this context, dispersion arises when surface wave velocity varies with wavelength or frequency. Dispersion in surface wave velocity occurs from changing stiffness properties of the soil and rock layers with depth. This phenomenon is illustrated in Figure 2 for a multi-layered solid. A high-frequency surface wave, which propagates with a short wavelength, only stresses material near the exposed surface and thus only samples the properties of the shallow, near-surface material (Figure 2b). A lower-frequency surface wave, which has a longer wavelength, stresses material to a greater depth and thus samples the properties of the shallower and deeper materials (Figure 2c). Spectral analysis is used to calculate the surface wave phase velocity at different frequencies (or wavelengths) to determine the experimental ("field") dispersion curve for the site (Figure 2d). An analytical procedure is then used to generate a dispersion curve for a one-dimensional layered system of varying layer stiffnesses and thicknesses [3]. An iterative procedure is employed to determine the one-dimensional $V_S$ profile that generates a dispersion curve which best matches the field dispersion curve. This best-match profile is presented as the $V_S$ profile of the site.

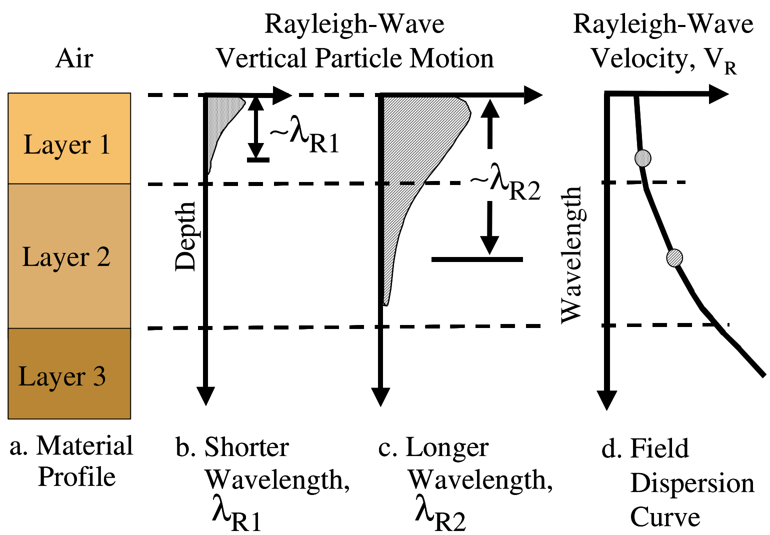


**Figure 2 Illustration of surface waves with different wavelengths sampling different materials in a layered system which results in dispersion in Rayleigh-wave velocity**

The SASW field procedure involves generating surface waves at one point on the exposed material surface and measuring the motions perpendicular to the surface created by the passage of the surface waves at two or more locations. All measurement points are arranged on the exposed surface along a single radial path from the source. The distance between the source and the first receiver is typically kept equal to the distance between receivers. Data are collected at shorter wavelengths (sampling material near the surface) by using small receiver spacings and a source capable of generating high frequencies. Longer wavelength data (sampling deeper material) are collected by using successively larger receiver spacings and correspondingly larger sources which generate lower and lower frequencies. Measurements are performed with several (typically seven or more) sets of source-receiver spacings, and the totality of seven or more sets of source-receiver spacings is called an SASW array.

An individual dispersion plot of surface wave phase velocity, $V_R$, versus wavelength, $\lambda_R$, is generated for each receiver pair from the frequency, $f$, unwrapped phase difference between the receivers, $\phi$, and the receiver spacing, $d$, using:

$$V_R = f \bullet \frac{360}{\phi} \bullet d \tag{1}$$

This surface wave velocity does not represent any single surface wave mode, but is an apparent velocity arising from the superposition of body and surface wave modes. Individual dispersion curves are generated for all source-receiver spacings used at the site. The SASW methodology is designed such that each wavelength range is generally covered by at least two individual dispersion curves. The individual dispersion curves from all receiver spacings are combined into a single composite dispersion curve called the experimental or field dispersion curve for the site. Continuous overlapping in adjacent dispersion curves provides confidence in the individual and composite curves and an indication that limited lateral variability exists at the site.

Once the composite dispersion curve is generated for the site, an iterative forward modeling procedure is used to create a theoretical dispersion curve to match this experimental curve [3]. The theoretical stiffness profile that provides the best match to the experimental dispersion curve is presented as the shear-wave velocity, $V_S$, profile at the site. Additional details of the SASW procedure can be found in Stokoe et al. [2].

## SUMMARY OF FIELD PROCEDURES USED ALONG THE TOP OF YUCCA MOUNTAIN

SASW measurements were performed at 22 array sites along the top of Yucca Mountain. These sites were spread over a distance of about 5 km. The majority of the array sites were located along and coincident with the gravelly road that traverses the crest of the mountain. The SASW measurements and results from these surveys are termed “parallel to the crest.” The remaining array sites were located within about 100 m of the road, but the arrays were oriented perpendicular to the road such that the receiver array ran eastward and down the slope for a maximum additional distance of about 100 m. These measurements are termed “perpendicular to the crest” in the following discussion.

### Equipment and Measurement Procedures for Deep Profiling

Of the 22 array sites, deep profiling was performed at 11 sites. At these sites, a Vibroseis source was used to generate the low-frequency surface waves necessary to profile to intermediate (about 100 m) and deep (about 200 m) depths. Seven arrays were oriented parallel to the crest on the mountain top. Four arrays were oriented perpendicular to crest. A typical SASW array for these measurements parallel to the crest included nine receiver spacings ranging from 1 to 244 m. At receiver spacings up to 8 m, a sledge hammer was used to excite the surface wave energy. At longer receiver spacings, the Vibroseis source was employed. The Vibroseis used in this study was owned by Lawrence Berkeley National Laboratory. Figure 3 is a photograph of the Vibroseis truck in operation. The Vibroseis has proven to be an ideal source of surface wave energy in previous work [4]. Ground motions were recorded using Mark Products Model L-4C transducers which have a natural frequency of 1 Hz. The key points with regard to these receivers are that: 1) they have significant output over the measurement frequency range generated with the Vibroseis (3 Hz to 100 Hz), 2) they are matched so that any differences in phase are negligible over the measurement frequency range, 3) they couple well to the soil, and 4) the coupling is similar for

**Figure 3 Photograph of Vibroseis truck in operation on the top of Yucca Mountain**

each receiver. The recording device used in this study was a Hewlett-Packard 3562A Dynamic Signal Analyzer. The dynamic signal analyzer was used to record the geophone output and to perform calculations in the frequency domain so that the relative phase (calculated from the cross-power spectrum between two channels) was reviewed at each receiver spacing during data collection. In addition, the Vibroseis was modified for this study so that the source output of the analyzer could be used to control the vibration frequency and amplitude of the Vibroseis.

The SASW measurements with the Vibroseis were performed in a swept-sine mode. The modifications to the Vibroseis allowed the signal analyzer to slowly sweep the source excitations over the frequencies of interest while simultaneous narrow-band filtering, which was centered on and swept with the input signal, was performed on the receiver outputs. This process optimized the input energy from the source at each frequency and allowed generated surface motions at each input frequency to be extracted from background noise at the receivers. The Vibroseis was controlled to remain at a single frequency until an acceptable coherence value (indicative of signal-to-noise ratio) was achieved. This procedure was performed over a frequency range from 100 Hz down to 2 Hz, although little energy was generated with the Vibroseis below about 3 Hz and no data were used below 3 Hz. Figure 4a shows the wrapped phase plot measured using the Vibroseis source and two receivers located 122 m apart. The individual dispersion curve calculated from this receiver spacing is shown in Figure 4b. The composite dispersion curve generated from all receiver spacings at this array location is shown in Figure 4c. The portion of the composite curve from the 122-m receiver spacing is highlighted in Figure 4c to demonstrate the excellent overlapping from adjacent receiver spacings.

Deep profiling (to a depth of approximately 200 m) was intended at 11 sites, but only six surveys reached depths ranging from 150 to 210 m. The other five surveys resulted in $V_S$ profiles averaging about 100-m deep. The limited profile depths of about 100 m were the result of problems and restrictions encountered in the field and not limitations of the methodology itself. For example, site access restrictions limited the locations of the Vibroseis resulting in shorter SASW array lengths and shallower profile depths. In addition, intermittent Vibroseis problems resulted in compromised low-frequency performance for a few of the array measurements before the problem was identified and rectified.

**Equipment and Measurement Procedures for Shallower Profiling**

Shallower profiles were measured at another 11 sites using a D-8 bulldozer as the surface wave source. This profiling was conducted to augment the deeper profiles and to study further a significant $V_S$ gradient close to the surface revealed in the deep profiling. Of the 11 shallower-profiling sites, six were oriented parallel to the crest and five were oriented perpendicular to the crest. The deepest profile achieved with the bulldozer source was 61 m and the average profile depth was about 45 m.

A typical array for measurements with the bulldozer source included six receiver spacings ranging from 1.5 to 61 m. A sledge hammer was used to excite the surface wave energy at small receiver spacings up to 8 m. At longer receiver spacings, the D-8 bulldozer was used. Unlike the Vibroseis, which could be operated at single frequencies and swept over a range in frequencies, the bulldozer generated band-limited random noise over a frequency range of approximately 75 Hz down to about 8 Hz. The bulldozer generated the surface wave energy by moving back-and-forth over a distance of approximately 5 m. Data were collected and averaged in the frequency domain until phase plots with strong trends and reasonable coherence were achieved. The geophones and recording equipment that were used with the Vibroseis measurements were used with the bulldozer measurements.

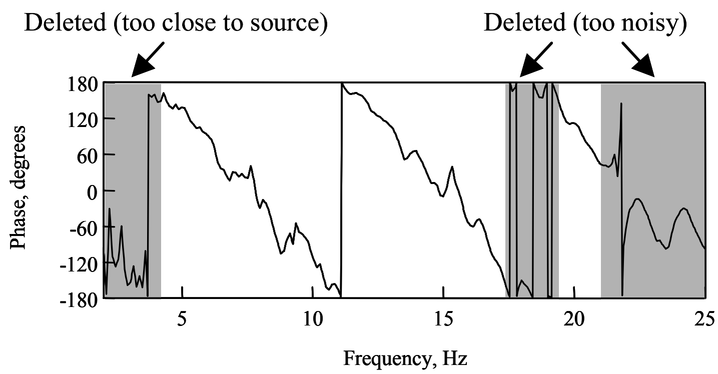


a. Phase plot from 122-m receiver spacing

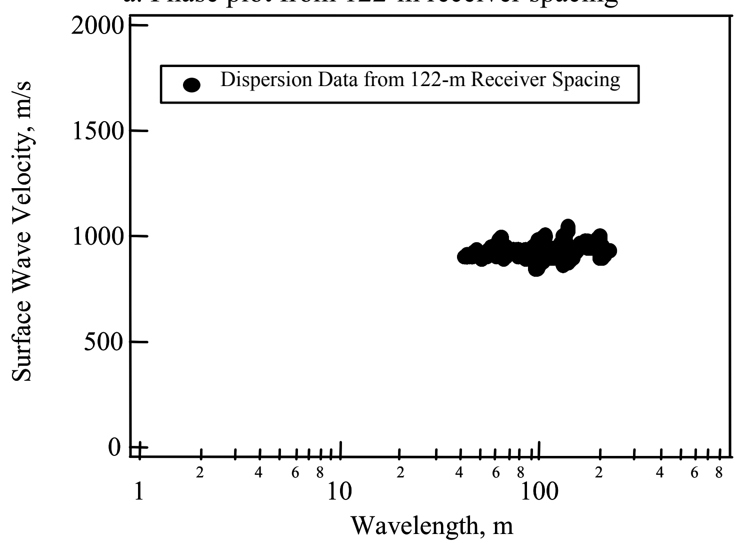


b. Individual dispersion curve calculated from the phase plot shown in Figure 4a

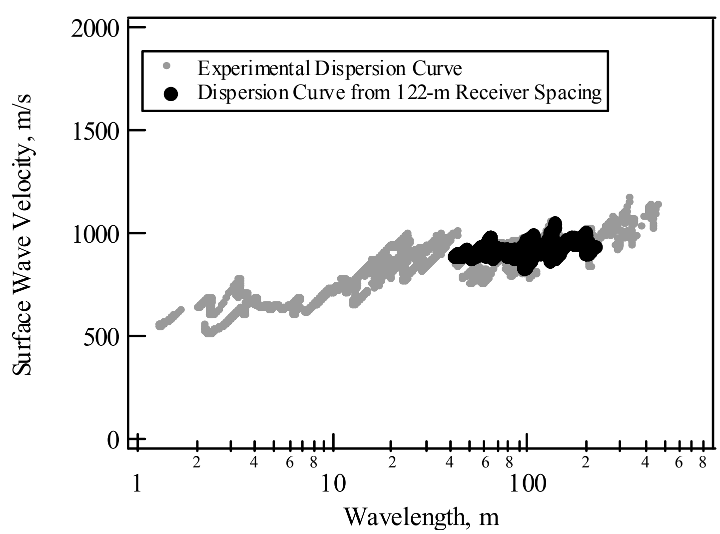


c. Composite dispersion curve calculated from receiver spacings of 1, 2, 4, 8, 15, 30, 61, 122, and 244 meters

**Figure 4 Field data from SASW measurements performed using the Vibroseis source**

## DATA REDUCTION AND FORWARD MODELING OF THE SASW FIELD MEASUREMENTS

The data collected in the field were interpreted in the office using the program WinSASW [3]. For each receiver spacing, the phase difference and coherence function were loaded into WinSASW. A masking procedure was performed to manually eliminate portions of the data with poor signal quality or portions of the data contaminated by near-field wave motions. Masked (deleted) regions are shown in the phase plot in Figure 4a. The program uses the masking information to unwrap the phase plot and calculate the dispersion curve using the relationship presented in Equation 1. The individual dispersion curve shown in Figure 4b was created after masking the phase plot. This masking process was repeated for all receiver spacings and resulted in a composite dispersion curve that covered a wide range of wavelengths as illustrated in Figure 4c for measurements performed with the Vibroseis source.

The next step in the data reduction procedure is the creation of the theoretical dispersion curve. The program WinSASW is also used for this purpose. WinSASW uses the stiffness matrix approach to generate a theoretical dispersion curve for a given $V_S$ profile [5]. The theoretical dispersion curve is generated using a complete solution which includes all modes and all body wave arrivals. An initial $V_S$ profile is assumed based on the characteristics of the measured experimental dispersion curve. The theoretical dispersion curve is generated and compared to the experimental curve. The $V_S$ profile features (velocities and layer thicknesses) are iteratively changed until an acceptable fit to the experimental curve is achieved. Figure 5a shows the final fit to the composite experimental dispersion curve shown in Figure 4c. Figure 5b shows the resulting $V_S$ profile determined for this site.

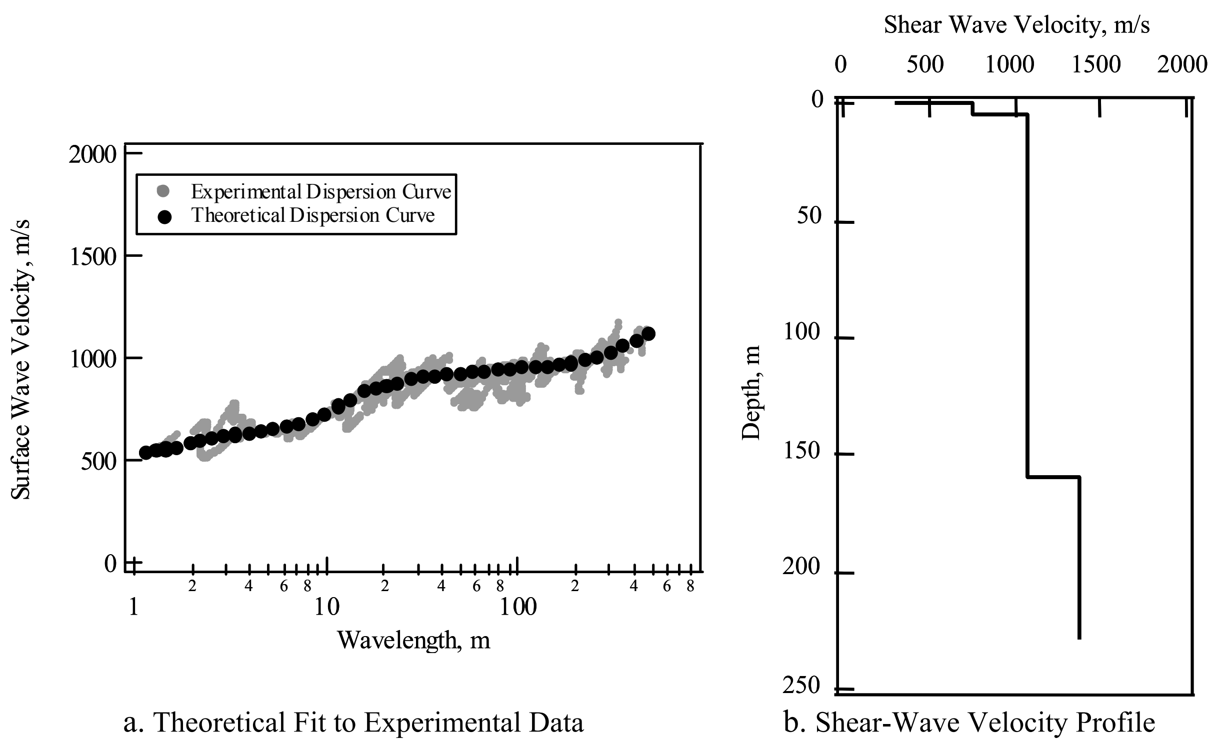


a. Theoretical Fit to Experimental Data b. Shear-Wave Velocity Profile

**Figure 5 Shear-wave velocity profile at one site from SASW measurements performed using the Vibroseis source**

To generate theoretical curves, some assumptions must be made. First, the unit weight and Poisson's ratio of the material must be assumed. Poisson's ratio was assumed to be 0.25 for all materials. This value of Poisson's ratio is a reasonable assumption when no water table exists in the profiling depth (as was the case here). When no water table is present, the value of Poisson's ratio (which may vary from 0.2 to 0.4) has only a minor influence (less than a few percent) on the calculated dispersion curve. The unit weight of the tuff was assumed to be 2.32 g/cm$^3$ at all depths. This value of unit weight was based on laboratory measurements of one rock type. Relative changes in unit weight with depth affect the dispersion curve, but the effect on the final shear wave velocity profile is very minor (less than a few percent). Therefore, precise knowledge of the unit weight values at all depths is not required.

In addition, the theoretical dispersion curve can be generated using different assumptions of source and receiver locations. For these analyses, the theoretical dispersion curve was calculated assuming a source-to-receiver-1 spacing of two wavelengths, and a source-to-receiver 2 spacing of four wavelengths. These receiver locations represent far-field motions. Past studies have shown that the range in wavelengths collected in the SASW test does not differ significantly from the far-field motions [6, 7, 8]. Lastly, the final $V_S$ profile is presented to a depth of approximately 0.5 times the maximum wavelength, $\lambda_{max}$, in these experimental dispersion curves. This cutoff depth is based on the theoretical solution for plane Rayleigh-wave propagation that shows most of the particle motion occurs at depths less than one-half of the wavelength, as illustrated in Figure 2. Past experience has shown this to be an acceptable cut-off depth for $V_S$ profiles as long as a significantly stiffer layer does not exist within the depth range of about 1.0 $\lambda_{max}$.

## DISCUSSION OF $V_S$ PROFILES ALONG THE TOP OF YUCCA MOUNTAIN

In 19 of the 22 surveys, a consistent experimental dispersion curve was measured to which a single theoretical dispersion curve was fit. At each of these 19 sites, therefore, a single $V_S$ profile was determined. At three array sites, the dispersion curves were inconsistent over some range in wavelengths. This lack of consistency in the dispersion curves between adjacent receiver spacings indicated significant lateral variability over the distance covered by the SASW receiver array. At these sites, multiple $V_S$ profiles (typically three) were required to account for the lateral variability. An average $V_S$ profile was determined at these three sites by averaging the individual $V_S$ profiles. These three average profiles were combined with the other 19 profiles to form the data set of 22 $V_S$ profiles used in this discussion and analysis.

All 22 $V_S$ profiles determined on top of the mountain are presented in Figure 6. The number of profiles at each depth is displayed to the right of the $V_S$ profiles. The number of profiles at each depth decreases from 22 within 25 m of the surface to three at a depth of 200 m. Examination of the individual $V_S$ profiles indicates a general trend of lower values near the surface with a rapid increase (up to $V_S$ values of 1500 m/s in some cases) followed by inversions at various depths in different profiles. This general trend of velocity inversions at depth is unlike the typical increase in velocity with depth observed in many geologic settings. However, such a pattern of low-velocity zones is observed in volcanic terrains where the velocities reflect varying degrees of welding in volcanic tuff (e.g. Jemez Caldera, New Mexico) or sedimentary layers interbedded with basalt (e.g. eastern Snake River Plain) [9].

A limited number of downhole measurements was also performed by another organization at five locations along the crest of Yucca Mountain [1]. A comparison of the $V_S$ profiles measured in the downhole surveys to the $V_S$ profiles measured in the SASW surveys is shown in Figure 7. Even though the downhole data are quite limited, both the downhole and SASW measurements produced $V_S$ profiles

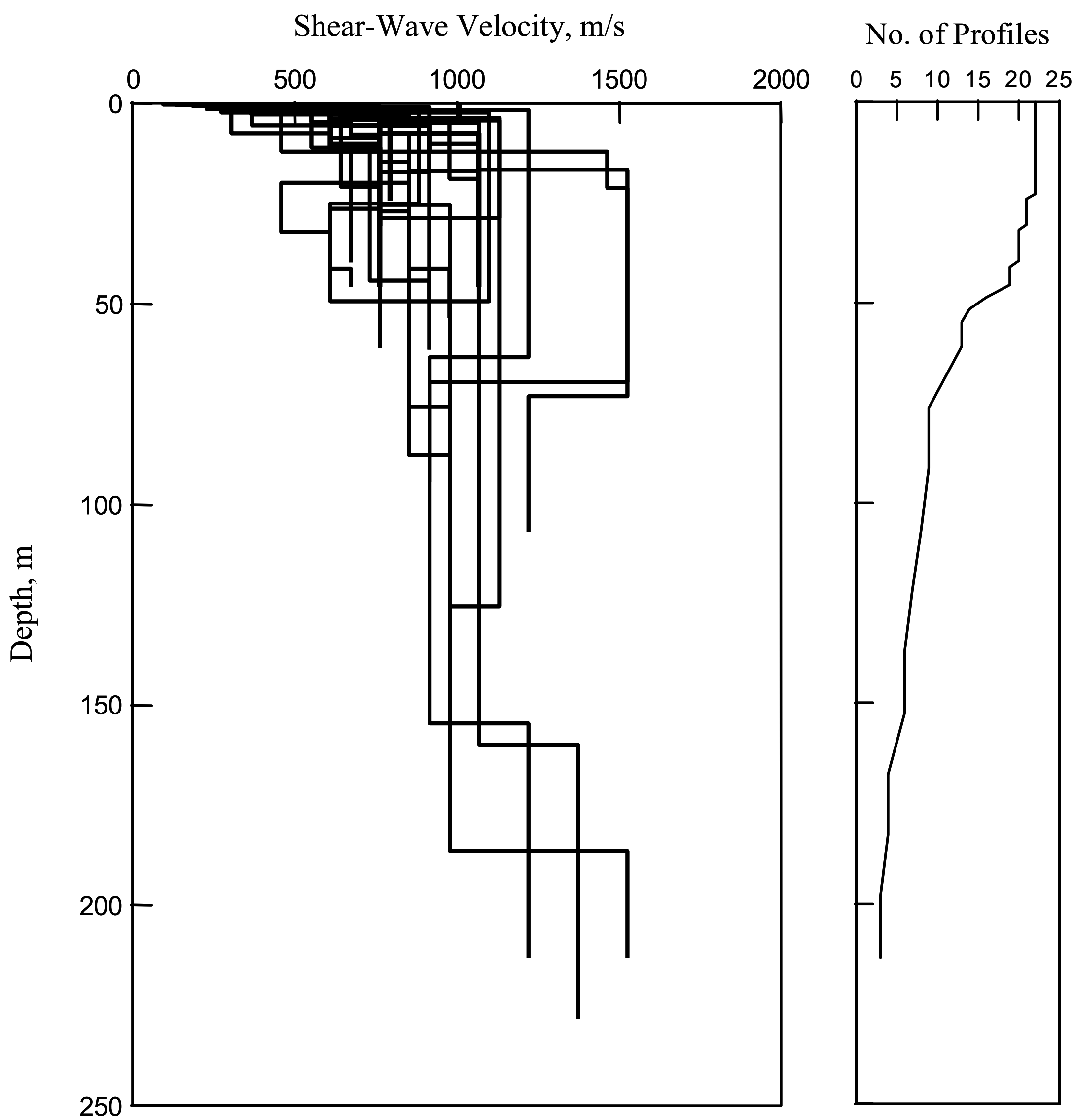


**Figure 6 Complete set of 22 $V_S$ profiles on top of Yucca Mountain**

that: (1) exhibit abrupt increasing and decreasing $V_S$ changes with depth, and (2) show a similar range in the $V_S$ values. Profiles determined from both types of measurements indicate regions of high $V_S$ values approaching 1500 m/s. The $V_S$ value of 1500 m/s is also consistent with very localized SASW measurements performed on intact rock outcrops on top of the mountain. These localized SASW measurements were performed specifically to evaluate the $V_S$ profile within exposed rock which, based on visual observation and tapping with a geologic hammer, was intact. The measurements were performed over a depth range of about 15 cm, and the $V_S$ values ranged from 980 to 1430 m/s.

The mean $V_S$ profile, determined from the 22 profiles, is presented in Figure 8 along with the $16^{th}$ and $84^{th}$ percentile $V_S$ values. The uncertainties and coefficient of variation (COV) about the mean profile were calculated by assuming the $V_S$ values follow a lognormal distribution. Several interesting trends are evident in Figure 8. First, it is observed that the near-surface $V_S$ gradient is quite abrupt. The values of

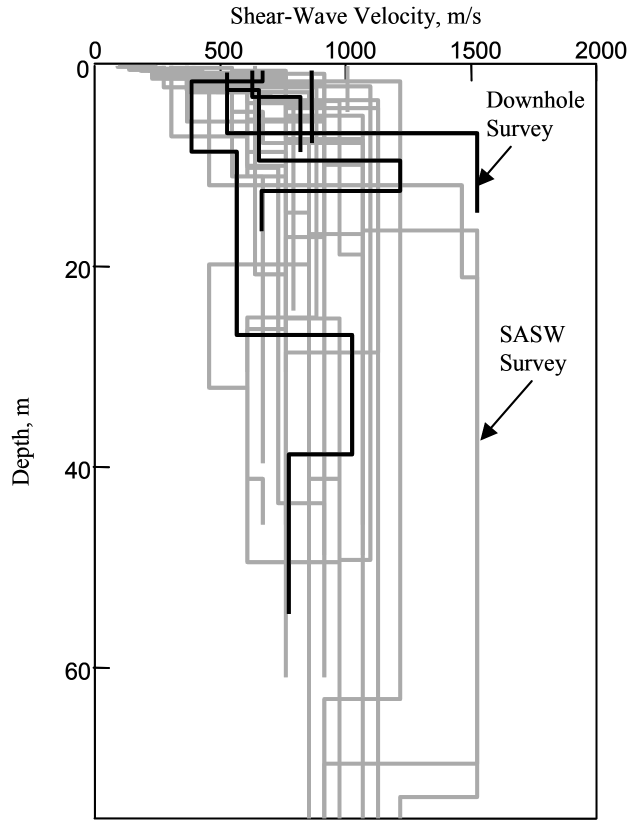


**Figure 7 Comparison of $V_S$ profiles in the top 60 m of Yucca Mountain from SASW and downhole measurements**

$V_S$ change from approximately 300 m/s in the top meter to over 800 m/s at a depth of only 5 m. Below 5 m, the mean $V_S$ value increases gradually from about 900 to 1000 m/s at a depth of 150 m. (It is interesting to note from Figure 1 that the depth of about 150 m corresponds to a change in rock type.) A gradient near the surface is expected due to the effects of weathering of the near-surface rock. The abruptness of the gradient, which has important implications in terms of the ground motion hazard, can not be predicted without field measurements of this kind. Sharp near-surface velocity gradients can result in the amplification of high-frequency ground motions, e.g. peak acceleration.

Another important result shown in Figure 8 is the nearly constant value of the mean $V_S$ below the 5-m-thick, near-surface zone. The measurements show a mean value of approximately 1000 m/s in the depth range of 10 to 150 m. This value of $V_S$ is on the low side of the range of 980 to 1430 m/s determined for intact exposed rock. These results illustrate the difference between local and global measurements of surface-wave velocity in a discontinuous rock/soil site with lateral variability. The maximum wavelength generated from the Vibroseis source was approximately 480 m. The maximum wavelength generated in the miniaturized SASW tests on intact rock in the field was on the order of 0.3 m. Although there are localized regions of intact, higher-velocity rock, the long wavelengths used in the deep SASW profiling measure the velocity of a large volume of material consisting of the matrix of rock, fractured rock, and infill material.

Another interesting feature in Figure 8 is the decrease in the value of the COV (standard deviation divided by the mean $V_S$) below a depth of approximately 60 m. It is expected that the spatial variability of the $V_S$ values will decrease with increasing profile depth due to the diminishing influence from surface

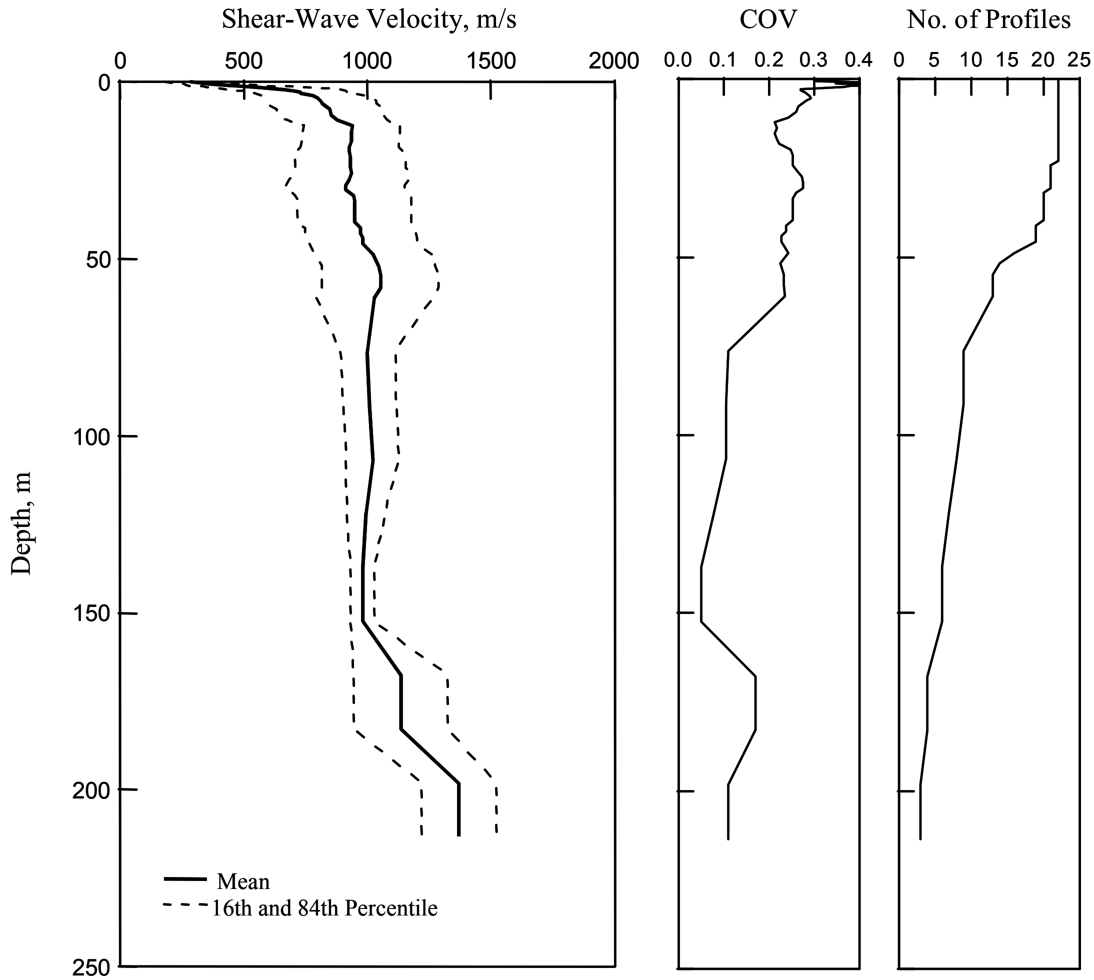


**Figure 8 Statistical analysis of $V_S$ profiles from SASW measurements on top of Yucca Mountain**

weathering and the increasing global extent of the SASW measurements with increasing profiling depth. However, much of the change in $V_S$ variability with depth can be explained by examining the effect of different array orientations on the average profiles. As mentioned earlier, 13 of the 22 arrays were oriented parallel to and along the crest of Yucca Mountain while nine arrays were oriented down the slope of the mountain, running approximately perpendicular to the crest. Due to site access issues, all but two of the profiles generated from arrays running down the slope only extended to maximum depths of 60 m or less. When the mean $V_S$ profiles are calculated separately for arrays oriented perpendicular to the crest and arrays oriented parallel to the crest, a clear distinction between the mean $V_S$ profiles is apparent. Figure 9 presents this comparison of mean $V_S$ profiles along with the $16^{th}$ and $84^{th}$ percentile profiles. The arrays oriented perpendicular to the crest show a mean $V_S$ value that is approximately 200 m/s less than the mean $V_S$ from parallel arrays in the depth range of 5 to 50 m. Over much of this depth range, the mean $V_S$ value from the arrays perpendicular to the crest is less than the $16^{th}$ percentile $V_S$ value from the parallel arrays. Clearly, anisotropy exists in the shear stiffness of the tuff, expressed by the different $V_S$ profiles in the two directions. Inclusion of this anisotropy in the top 50 m results in greater variability than measured in the data at greater depths which were all collected with arrays oriented parallel to the crest. Figure 10 presents the dispersion data for measurements in both directions with wavelengths up to 120-m long. The data in Figure 10 were used to determine the $V_S$ profiles in the top 60 m. Each dispersion curve shown by the symbols is an average curve that was developed by

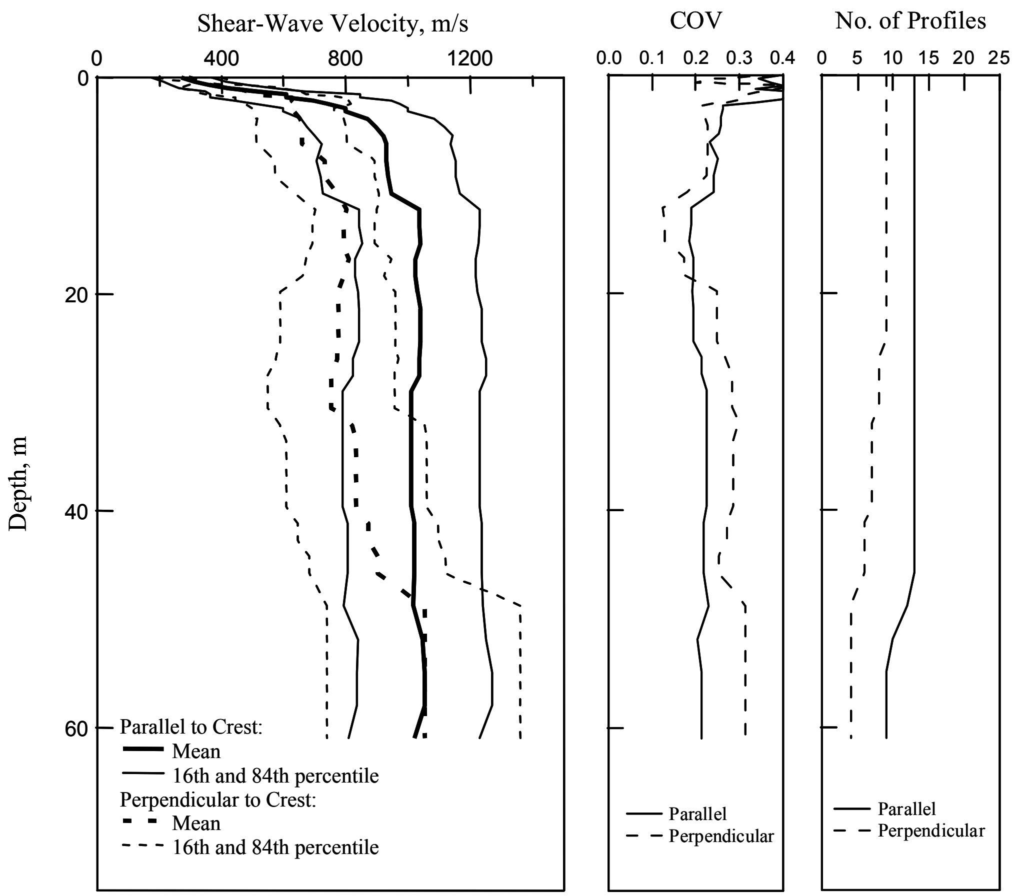


**Figure 9 Statistical analysis of $V_S$ profiles from SASW measurements performed parallel to and perpendicular to the crest of Yucca Mountain**

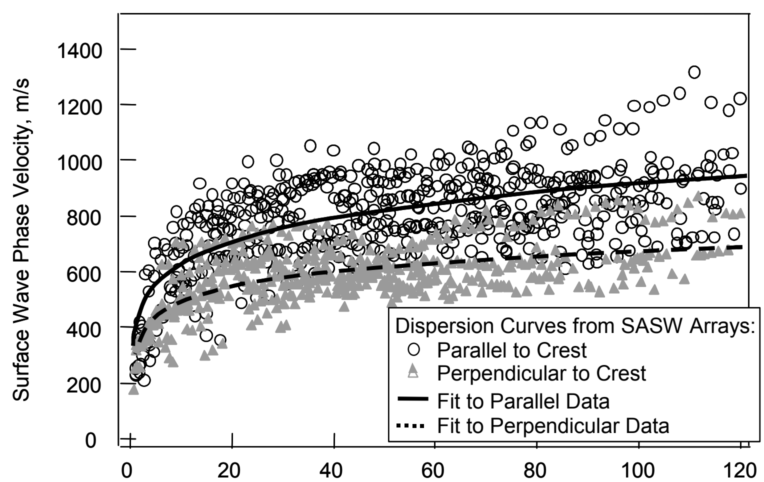


**Figure 10 Anisotropy in the $V_S$ structure shown in the dispersion curves measured in different directions on top of Yucca Mountain**

representing the trend in each composite dispersion curve with approximately 50 points in the wavelength range of interest. The difference in surface-wave velocities for measurements parallel and perpendicular to the mountain crest is clearly shown in these data, which represent raw data before any inversion is performed. The general trend lines that are fit to the data sets in Figure 10 highlight the anisotropy.

The difference in the mean $V_S$ profiles parallel and perpendicular to the crest, may be related to anisotropy due to fracturing in the near-surface volcanic units of Yucca Mountain. The dominant fracture pattern is oriented parallel to the crest and thus velocity measurements perpendicular to the crest are being made across fractures. We speculate that this could result in the lower velocities. Below a depth of 50 m, there are few deep profiles perpendicular to the crest to make a valid comparison. However, it appears from the limited profiles available that the mean $V_S$ profile from the perpendicular arrays increases to about the same mean $V_S$ profile as the parallel arrays below 50 m. This suggests to us that the effect of fracturing is not significant below 50 m, either due to the absence of fracturing or possibly due to the effect of confining pressure

## CONCLUSIONS

SASW measurements were successfully performed on the top of Yucca Mountain to evaluate $V_S$ profiles to a maximum depth of 210 m. This profiling depth represents the deepest profiles ever measured with the SASW method. Deep profiling was possible because of the following three factors: (1) a large vertical shaker, a Vibroseis, was used as the surface-wave source, (2) the Vibroseis was modified so that a signal analyzer could be used to create slow frequency sweeps with the Vibroseis, which allowed the shaker output to be maximized in the 3 to 8 Hz range, and (3) the layers of tuffs have a mean $V_S$ slightly above 1000 m/s in the upper 200 m which allowed wavelengths as long as 480 m to be measured and permitted profiling to the maximum 210-m depth.

Statistical analyses of the 22 $V_S$ profiles measured on top of the mountain revealed several interesting results. First, there is a strong velocity gradient within 5 m of the rock surface, with the mean value of $V_S$ increasing from about 300 to 800 m/s in this depth range. The strong gradient is attributed to decreasing fracturing and weathering with depth in the tuff. Second, the mean $V_S$ only changes slightly in the 10- to 150-m depth range, from about 900 to 1000 m/s. Third, between depths of 150 and 210 m, $V_S$ increases more rapidly to about 1350 m/s, but this trend is based on limited data. Fourth, additional statistical analyses were performed on the $V_S$ profiles within 60 m of the surface which revealed an anisotropic $V_S$ structure at depths less than 50 m. These analyses were possible because of additional shallower SASW profiling performed with a bulldozer source and because profiling was conducted along the crest and perpendicular to the crest using both the Vibroseis and bulldozer sources. The average $V_S$ values in the 5- to 50-m depth range were about 200 m/s less for measurements oriented perpendicular to the crest than parallel to the crest. We speculate that this difference in velocities is due to the differing effects on the surface waves traveling parallel to versus perpendicular to the trend of fractures in the shallow portion of Yucca Mountain. Finally, the average COV of all data is about 0.25 in the 5- to 50-m depth range. Below 75 m, where the data set is smaller and anisotropy is not included, the average COV decreases to about 0.11. These COV values are well below the value of 0.40 often attributed to large data sets of $V_S$ profiles for generic rock [10]. The lower COV values are attributed to: (1) measurements in a relatively small area, (2) significant averaging at depth inherent in the SASW measurements, and (3) measurements in only one geologic setting.

## ACKNOWLEDGEMENTS

The studies described in this paper were performed for the Department of Energy under Prime Contract DE-AC08-01NV12101 to Bechtel-SAIC Company, LLC. We wish to acknowledge the assistance of many individuals including Mike Luebbers, Rob Lung, Steven Beason, Mark Esp, Drew Coleman, Cliff Howard, Mark Dober, and Richard Pernisi. A special thanks is given to Alicia Zapata for assisting in the preparation of this paper.

## REFERENCES

1. BSC (Bechtel-SAIC LLC.). "Development of earthquake ground motion input for preclosure seismic design and postclosure performance assessment of a geologic repository at Yucca Mountain, Nevada, unpublished report prepared by URS Corporation, Rev. 00, 2003.
2. Stokoe, K.H., II, Wright, S.G., Bay, J.A. and J.M. Roesset. "Characterization of geotechnical sites by SASW method," ISSMFE Technical Committee 10 for XIII ICSMFE, Geophysical Characteristics of Sites, A.A. Balkema Publishers/Rotterdam & Brookfield, Netherlands, pp. 785-816, 1994.
3. Joh, S.-H.. "Advances in interpretation and analysis techniques for spectral-analysis-of-surface-waves (SASW) measurements," Ph.D. Dissertation, The University of Texas at Austin, 240 pgs, 1996.
4. Andrus, R.D., Chung, R.M., Stokoe, K.H., II and Bay, J.A. "Delineation of densified sand at Treasure Island by SASW testing," First International Conference on Site Characterization, Atlanta, Georgia, April, 6 pgs, 1998.
5. Kausel, E. and Roesset, J. M. "Stiffness matrices for layered soils," Bull. Seismol. Soc. Am., 71, pp. 1743-1761, 1981.
6. Foinquinos M. R. "Analytical study of inversion for the spectral-analysis-of-surface-waves method," Master's Thesis, The University of Texas at Austin, 119 pgs, 1991.
7. Roesset, J.M., Chang D.-W., and Stokoe, K.H., II. "Comparison of 2D and 3D models for analysis of surface wave tests," Proceedings of the 5th International Conference on Soil Dynamics and Earthquake Engineering, pp. 111-126, 1991.
8. Sanchez-Salinero, I. "Analytical investigation of seismic methods used for engineering applications," Ph. D. Dissertation, The University of Texas at Austin, 401 pgs, 1987.
9. Wong, I., Kelson, K., Olig, S., Kolbe, T., Hemphill-Haley, M., Bott, J. Green, R., Kanakari, H., Sawyer, J., Silva, W.J. Stark, C., Haraden, D., Fenton, C., Unruh, J. Garner, J., Reneau, S. and House L., "Seismic hazard evaluation of the Los Alamos National Laboratory," unpublished report prepared for LANL by Woodward-Clyde Federal Services, 1995.
10. Silva, W.J., Abrahamson, N., Toro, G. and Costantino, C. "Description and validation of the stochastic ground motion model," unpublished report prepared by Pacific Engineering and Analysis for the Brookhaven National Laboratory, 1996.